図5　T2マッピングによる膝関節軟骨変性の評価
カラーバーの赤色はT2の長い変性部位を，青色はT2の短い健常部位を示している。

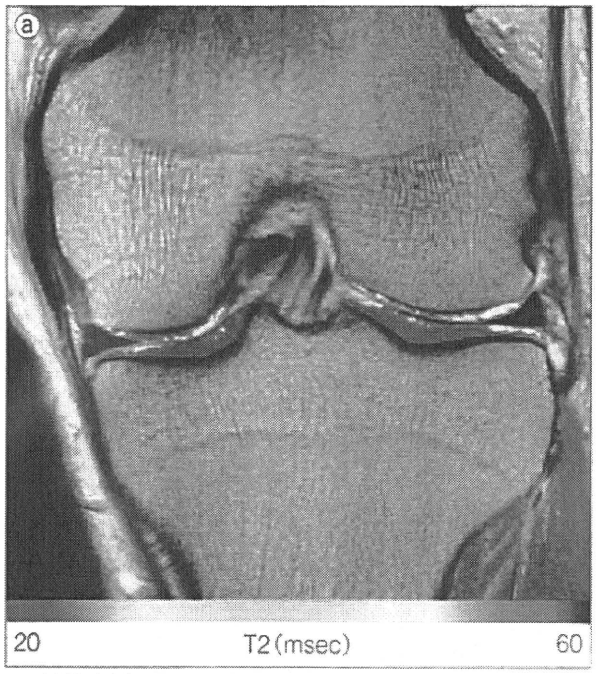

a：健常症例のT2マッピング冠状断像
健常症例のT2マッピング像では，関節軟骨は均一で比較的短いT2で示される。

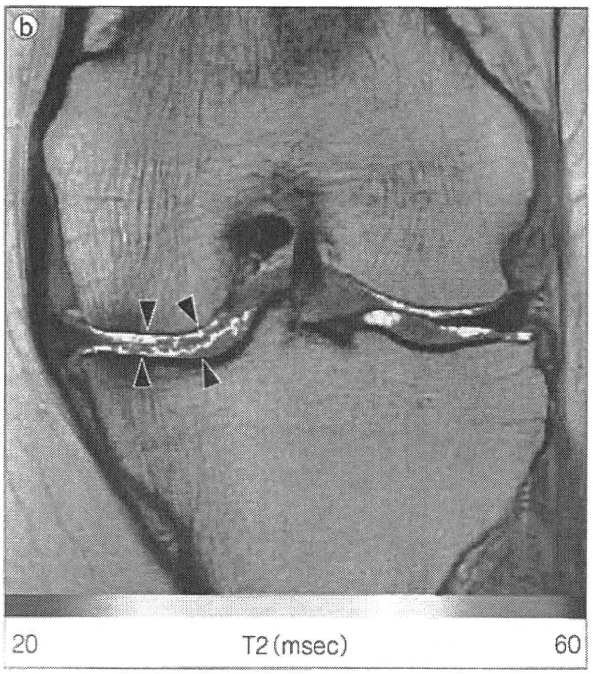

b：Kellgren-Lawrence分類GradeⅡと分類された内側型膝OA症例のT2マッピング冠状断像
50歳代，女性。大腿骨内側顆および脛骨内側顆の軟骨表層から深層にかけて広範なT2延長が認められ(▲)，コラーゲン配列の不整化や水分含有量の上昇などを伴う軟骨変性が示唆される。

拡散し，撮像時には軟骨全層に安定した拡散が得られる。

dGEMRICではT1計算画像を作成し，GAG濃度の違いをT1の差として定量化するが，一般にはinversion recovery法を用いたsingle slice撮像によるT1測定が行われる。その他3D撮像によるT1測定も行われているが，空間分解能の制限や，repeatabilityの低下などが知られる[6]。

臨床診断の際にはT1計算画像中の軟骨部分を抽出し，T1に基づいてカラーコーディングした画像を作成して視覚的な評価を行っている。またより詳細な定量的評価が必要な場合には，T1計算画像上に関心領域を設定してT1を測定している。

T2マッピング(図5)

T2マッピングは，軟骨中のコラーゲンの配列と水分含有量が評価可能なMRI撮像法であり，dGEMRICと同様に早期軟骨変性の検知や軟骨変性度の定量的評価に有用とされる。正常軟骨は密で規則的に配列するコラーゲンを有し，また水分含有量はほぼ一定に保たれているが，軟骨変性に伴いコラーゲン配列の不整化や水分含有量の増加が進行する。これらの変化はともにT2を延長させるため，変性の進行に従って軟骨のT2は延長する。T2マッピングではT2計算画像を作成し，コラーゲン配列や水分含有量の違いをT2の差として定量化するが，一般にはmulti-spin-echo法を用いたsingle slice撮像によるT2測定が行われる。その他multi-slice撮像によるT2測定も行われるが，SNRの低下やこれに伴うT2の測定誤差を生じる可能性がある[7]。

臨床診断にはT2に基づいてカラーコーディングした画像による視覚的評価を，詳細な定量的評価にはT2計算画像上に関心領域を設定したT2測定を行っている。

図6　T1rhoマッピングによる膝関節軟骨変性の評価
カラーバーの赤色はT1rhoの長い変性部位を，青色はT1rhoの短い健常部位を示している。

a：健常症例の冠状断T1rhoマッピング像
健常症例のT1rhoマッピング像では，関節軟骨は均一で比較的短いT1rhoで示される。

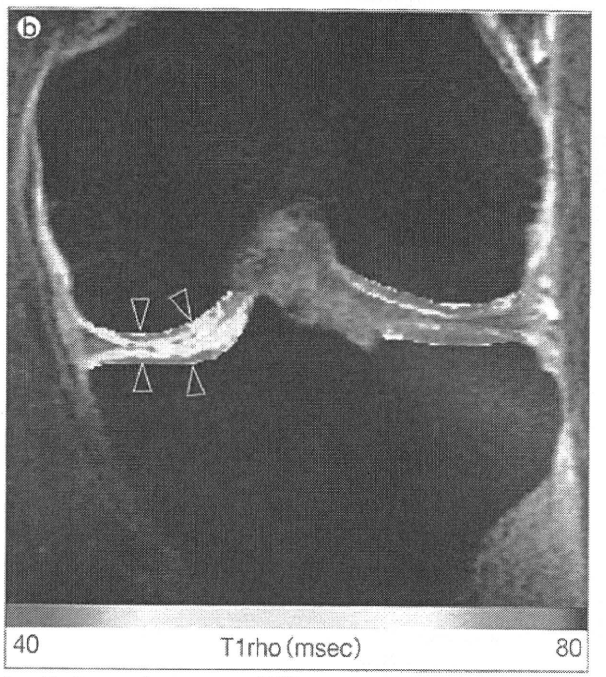

b：Kellgren-Lawrence分類Grade Ⅰと分類された内側型膝OA症例のT1rhoマッピング冠状断像
40歳代，女性。大腿骨内側顆および脛骨内側顆の軟骨表層から深層にかけて広範なT1rho延長が認められ(▲)，GAG濃度の低下や水分含有量の上昇などを伴う軟骨変性が示唆される。

T1rhoマッピング(図6)

T1rho(spin-lattice relaxation in the rotating frame)マッピングは，軟骨中のGAG濃度の評価が可能なMRI撮像法とされる[8]。dGEMRICと比較し造影剤の投与が必要ないため，より非侵襲的な評価が可能である。一方dGEMRICによるT1の変化は，GAG濃度の変化に特異性が高いが，T1rhoマッピングによるT1rhoの変化は，GAGだけでなく水分含有量やコラーゲン配列の変化などにも影響を受けることが知られる[9,10]。変形性関節症(osteoarthritis；OA)の早期に生じる軟骨中のGAG濃度の低下，水分含有量の増加，コラーゲン配列の不整化はともにT1rhoを延長させることから，T1rhoマッピングは早期軟骨変性の有効な指標となるが，いずれのパラメータにも特異性は低いと考えられる。

T1rhoマッピングでは，T1rho計算画像を作成し軟骨変性度を定量化するが，最近は各社から3D T1rhoマッピングの撮像シーケンスが提供されていることもあり，空間分解能などに制限はあるものの，3D撮像によるT1rho測定が行われることが多い[9]。臨床診断にはT1rhoに基づいてカラーコーディングした画像による視覚的評価を，詳細な定量的評価にはT1rho計算画像上に関心領域を設定したT1rho測定を行っている。

UTE MRI

組織はさまざまなT2をもつ構成要素からなるが，T2の短い要素からのmagnetizationは，TEが十分に短くないと評価できない。ultrashort echo time MRI(UTE MRI)は，きわめて短いTEを用いることにより，通常用いられるTEでは検知困難な，組織中のT2の短いコンポーネントの評価が可能なMRI撮像法である[11]。

表1　OAI MRIプロトコル

No.	スキャン
1	localizer (3-plane)
2	sagittal 3D dual-echo steady-state WE
3	coronal IW TSE FS
4	sagittal IW TSE FS
5	coronal T1 3D fast low-angle shot WE
6	sagittal T2 mapping

OAI：osteoarthritis initiative, 3D：three-dimensional, WE：water excited, IW：intermediate-weighted, TSE：turbo spin-echo, FS：fat-suppressed

この方法は骨軟部領域では，半月板，皮質骨，骨膜，腱，靱帯などの病変の評価に用いられるが，関節軟骨ではその最深層にある石灰化層の描出が可能である。石灰化層はOAの初期より変化がみられることが知られており[12]，UTE MRIは初期OAの検知に有用と期待されている。しかしUTE MRIにより捉えられる変化の病的意義などに関してはいまだ不明な点も多く，データの蓄積が必要である。

OAI

Osteoarthritis Initiative(OAI)は，非常にユニークな現在全米の多施設で行われている膝OAの前向き研究(prospective study)，および縦断研究(longitudinal study)である(http://www.oai.ucsf.edu/datarelease/)。OAは，成人において日常生活動作(ADL)の障害の最も一般的な原因となることから，National Institutes of Health(NIH)がスポンサーになって，同疾患の予防と治療の研究を促進するため，現在4年間の観察研究(observation study)を行っている。

この研究のユニークな点は，同疾患の発現や進行を理解するために，画像やバイオマーカー，臨床データなどをすべて公有にして，一般の研究者に公開している点にある。45～79歳の男女約5,000人がこの研究に参加しており，きわめて大規模な研究である。画像に関しては，膝の単純X線写真とMRIを毎年延べ4年間にわたって経過観察することになっており，今年(2010年)3月には，ベースライン，12カ月，24カ月，36カ月のMRIが公開された。MRIは3Tを使用しており，通常膝関節の撮像に使われる2D FSE法のほかに，3D-DESSやT2 mappingのパルスシーケンスが含まれている(表1)。これらの画像データは，OAIに登録し，データユーザー同意書にサインをするだけで利用することができる。実際には，データが十分に収まる容量のハードドライブを研究参加施設の1つであるUniversity of California, San Francisco(UCSF)の担当者に送ると，4～6週以内にデータをコピーして送り返してくれる。また必要なデータ量が少ないときは，UCSFですでに保有しているハードドライブを貸し出してくれ，こちらでコピーし終わったらUCSFに送り返すシステムになっている。

いずれにしても，何百人もの均一なフォローアップデータを，ハードドライブのやり取りだけで簡単に手に入れることができるのは，すばらしいシステムであり，1つの小さな施設では，それほどの数のデータを集めるには，お金も時間もかかるが，公有化により，アイデアさえあればそれらのデータを使ってどんどん研究することができる。OAIのホームページには，データはworld-wideに利用可能であると書いてあるので，興味のある方は，OAIに一度連絡してみてはいかがだろうか。

1) Collins CM, et al : Signal-to-noise ratio and absorbed power as functions of main magnetic field strength, and definition of "90 degrees" RF pulse for the head in the birdcage coil. Magn Reson Med, 45 : 684-691, 2001.

2) Gold GE, et al : Isotropic MRI of the knee with 3D fast spin-echo extended echo-train acquisition(XETA) : initial experience. AJR Am J Roentgenol, 188 : 1287-1293, 2007.

3) Jung JY, et al : Diagnosis of internal derangement of the knee at 3.0-T MR imaging : 3D isotropic intermediate-weighted versus 2D sequences. Radiology, 253 : 780-787, 2009.

4) Bashir A, et al : Nondestructive imaging of human cartilage glycosaminoglycan concentration by MRI. Magn Reson Med, 41 : 857-865, 1999.

5) Burstein D, et al : Protocol issues for delayed Gd (DTPA) (2−) -enhanced MRI (dGEMRIC) for clinical evaluation of articular cartilage. Magn Reson Med, 45 : 36-41, 2001.

6) Siversson C, et al : Repeatability of T1-quantification in dGEMRIC for three different acquisition techniques : two-dimensional inversion recovery, three-dimensional look locker, and three-dimensional variable flip angle. J Magn Reson Imaging, 31 : 1203-1209, 2010.

7) Watanabe A, et al : Effect of multislice acquisition on T1 and T2 measurements of articular cartilage at 3T. J Magn Reson Imaging, 26 : 109-117, 2007.

8) Wheaton AJ, et al : Correlation of T1rho with fixed charge density in cartilage. J Magn Reson Imaging, 20 : 519-525, 2004.

9) Taylor C, et al : Comparison of quantitative imaging of cartilage for osteoarthritis : T2, T1rho, dGEMRIC and contrast-enhanced computed tomography. Magn Reson Imaging, 27 : 779-784, 2009.

10) Burstein D, et al : Measures of molecular composition and structure in osteoarthritis. Radiol Clin North Am, 47 : 675-686, 2009.

11) Robson MD, et al : Magnetic resonance : an introduction to ultrashort TE(UTE) imaging. J Comput Assist Tomogr, 27 : 825-846, 2003.

12) Burr DB : Anatomy and physiology of the mineralized tissues : role in the pathogenesis of osteoarthrosis. Osteoarthritis Cartilage, Suppl A : S20-30, 2004.

Loaded Cartilage T2 Mapping in Patients with Hip Dysplasia[1]

Takashi Nishii, MD
Toshiyuki Shiomi, MD
Hisashi Tanaka, MD
Youichi Yamazaki, MS
Kenya Murase, PhD
Nobuhiko Sugano, MD

Purpose: To evaluate the change in cartilage T2 values with loading in patients with hip dysplasia.

Materials and Methods: Fifteen patients with hip dysplasia and nine asymptomatic healthy volunteers were evaluated between April 2008 and February 2009. All subjects provided written informed consent before participation in this prospective, institutional review board–approved study. Midcoronal T2 mapping of hips was performed under unloaded and loaded conditions (with 50% body weight) at 3.0-T magnetic resonance (MR) imaging. Loading was achieved with a mechanical loading system. T2 values under unloaded conditions and the change in T2 values at the weight-bearing area of the acetabular and femoral cartilage with loading were compared between normal and dysplastic hips. The change in T2 with loading was correlated with the patient's age and body mass index as well as with the center-edge angle determined on conventional radiographs.

Results: The decrease in cartilage T2 at the outer superficial zones of the acetabular cartilage with loading was significantly greater in patients with hip dysplasia than in healthy volunteers: The mean T2 change with loading was −7.6% ± 10.6 (±standard deviation) for dysplastic hips and 1.2% ± 10.9 for normal hips (P = .04). Among patients with hip dysplasia, there was a positive correlation between the center-edge angle on anteroposterior radiographs and T2 changes with loading at the outer deep zones of the acetabular cartilage.

Conclusion: Cartilage T2 mapping with loading during MR imaging enabled the detection of site-specific changes in cartilage T2 in dysplastic hips.

[1] From the Departments of Orthopaedic Medical Engineering (T.N., N.S.), Orthopaedic Surgery (T.N., T.S., N.S.), Radiology (H.T.), and Medical Physics and Engineering, Division of Medical Technology and Science, Faculty of Health Science (Y.Y., K.M.), Osaka University Graduate School of Medicine, 2-2 Yamadaoka, Suita, Osaka 565-0871, Japan. Received October 20, 2009; revision requested December 15; revision received February 17, 2010; accepted March 11; final version accepted March 16. Supported in part by a Grant-in-Aid for Scientific Research from the Ministry of Education, Science, and Culture of Japan. **Address correspondence to** T.N. (e-mail: *nishii@ort.med.osaka-u.ac.jp*).

Hip dysplasia is characterized by insufficient acetabular coverage of the femoral head and is a major cause of hip osteoarthritis (1,2). An abnormal biomechanical environment with elevated contact pressure on the area with limited cartilage is assumed to play a role in the progression of osteoarthritis in patients with hip dysplasia (3–5). Before osteoarthritis progresses, joint-preserving treatments such as weight loss, exercise, and pelvic osteotomy surgery are effective in reducing symptoms and limiting progression (6,7). Thus, it is important to accurately identify patients who are at high risk of osteoarthritis progression and apply joint-preserving treatments for hip dysplasia at a preosteoarthritic or early osteoarthritic stage.

Several morphologic indexes on plain radiographs are widely used to quantify the morphologic characteristics of osteoarthritis, including the center-edge angle, Sharp angle, and acetabular head index (8–10). Although these bone morphologic assessments are related to biomechanics, their prognostic value for estimating osteoarthritic progression is limited (2). Several investigators have used computational-mathematical analysis, including the rigid spring model (11,12) and finite element analysis (13–16), to estimate the biomechanical conditions of hip articular cartilage. To our knowledge, however, no biomechanical analysis can enable direct evaluation of load distribution on the cartilage of the hip joint in vivo.

The load responsiveness of articular cartilage has been experimentally studied by using magnetic resonance (MR) imaging and excised cartilage-bone plugs (17,18), and site-specific signal intensity changes along the cartilage depth were observed in response to the magnitude of applied compression force. This change in signal intensity is assumed to be caused by water extrusion or a change in the collagenous structure within the cartilage (17,19). Currently, several quantitative MR imaging techniques for cartilage assessment have been developed, including delayed gadolinium-enhanced MR imaging of cartilage and T2, T1ρ and sodium MR imaging, and diffusion-weighted MR imaging (20–22). The findings of these examinations correlate with changes in the cartilage's extracellular matrix, including changes in proteoglycans, collagen, and water (19–24).

We hypothesized that comparison between quantitative MR parameters under unloaded and loaded conditions in vivo could be useful in detecting a critical cartilage area with elevated contact pressure by enabling quantitative evaluation of the change of collagenous architecture or of the water influx or efflux of the cartilage (19,23,24). Hence, we developed a loading apparatus that applies an axial load to the hip joint during MR imaging to simulate physiologic load-bearing conditions upon standing. Among the quantitative MR imaging techniques for cartilage assessment, we chose T2 mapping because (*a*) T2 has shown a close correlation with collagenous architecture and water content (23,24) and (*b*) there is a zone-specific change in T2 along the cartilage depth in response to external loading (18). The purpose of this study was to examine the change in T2 maps with loading during MR imaging to detect site-specific changes in cartilage T2 in patients with hip dysplasia.

Advance in Knowledge

- Loaded cartilage T2 mapping showed that patients with hip dysplasia had a significantly larger decrease of cartilage T2 at the outer superficial zones of the acetabular cartilage compared with healthy volunteers.

Materials and Methods

Institutional review board approval was obtained for this study, and all subjects provided written informed consent after the nature of the procedure had been fully explained.

Implication for Patient Care

- Loaded cartilage T2 mapping with use of in situ MR imaging enables the detection of site-specific changes in cartilage T2 with loading in dysplastic hips.

Study Population

Nine healthy volunteers (nine hips) and 15 patients with hip dysplasia (15 hips) were included in this study between April 2008 and February 2009. Because most patients with hip dysplasia are women (25), men were excluded from this study to prevent the potentially confounding influence of sex on T2 mapping of articular cartilage (26). Volunteers were excluded if they were currently experiencing or had previously experienced hip pain, stiffness, limitation in the range of hip motion, or gait disability. Patients with hip dysplasia were included if they had not previously undergone hip surgery and had a center-edge angle of 24° or less on anteroposterior radiographs (27). Patients were also included if they had a class I subluxation (<50%) according to the classification used by Crowe et al (28) and preosteoarthritis or early radiologic osteoarthritis according to the Kellgren-Lawrence classification (29) of grade 0 (no osteoarthritic finding), grade 1 (possible narrowing of joint space and/or osteophytes), or grade 2 (definite narrowing of joint space, definite osteophytes, and slight sclerosis). In a previous study (30), the Kellgren-Lawrence classification of hip osteoarthritis was determined to provide sufficient interobserver reproducibility and

Published online
10.1148/radiol.10091928

Radiology 2010; 256:955–965

Abbreviations:
ROI = region of interest
WOMAC = Western Ontario and McMaster Universities

Author contributions:
Guarantors of integrity of entire study, T.N., N.S.; study concepts/study design or data acquisition or data analysis/interpretation, all authors; manuscript drafting or manuscript revision for important intellectual content, all authors; manuscript final version approval, all authors; literature research, T.N., T.S., Y.Y.; clinical studies, T.N., N.S.; statistical analysis, T.N., H.T., K.M.; and manuscript editing, T.N., N.S.

Authors stated no financial relationship to disclose.

reliable validity with regard to the relationship between clinical symptoms and the prediction of total hip surgery. At entry into this study, the Kellgren-Lawrence score was determined by one observer (N.S.), an orthopedic surgeon with more than 20 years of experience in the treatment of hip osteoarthritis.

The average ages of the volunteers and patients were 28 years (range, 23–40 years) and 39 years (range, 24–50 years), respectively. The average weight and body mass index were 53 kg (range, 47–59 kg) and 20.8 kg (range, 18.9–23.2), respectively, for the volunteers and 56 kg (range, 43–70 kg) and 21.9 kg (range, 18.9–29.5), respectively, for the patients. There were no significant differences between the volunteers and patients with respect to weight and body mass index; however, the volunteers were significantly younger than the patients with hip dysplasia ($P = .004$).

At study entry, the center-edge angle of patients was measured on anteroposterior radiographs by one observer (N.S.). The center-edge angle, as measured on radiographs, ranged from −10° to 16° (mean, 4.7°). Six hips were classified as being in the prearthritic stage (grade 0), and nine were classified as being in the early arthritic stage (grade 1 or 2). Three patients had no pain in their hips, and 12 patients had slight or moderate pain in their hips either while walking or after a long walk. The volunteers did not undergo radiography. The center-edge angle of both patients and volunteers was measured on midcoronal MR images by one observer (N.S.). The interval between measurements performed on MR images and measurements performed on radiographs was at least 1 month. All volunteers had center-edge angles of more than 25° (range, 26°–34°) on midcoronal MR images. In patients, the center-edge angles on midcoronal MR images ranged from −8° to 17° (mean, 5°).

Clinical symptoms of the hip were evaluated in all participants by using the pain score of the Western Ontario and McMaster Universities (WOMAC) osteoarthritis questionnaire (31). The WOMAC pain score was calculated as the summation of the scores ranging from 0 (no pain) to 4 (extreme pain) in response to each of the five items (total score range, 0–20). The WOMAC score was determined by one musculoskeletal clinician (N.S).

MR Imaging

Patients and volunteers were instructed to limit strenuous weight-bearing activity (eg, running or ascending stairs for a long distance) 3 hours before MR imaging. All subjects were instructed to sit on a chair for at least 20 minutes before MR imaging. A unilateral hip joint was imaged under loaded and unloaded conditions by using a 3.0-T MR unit with a flexible surface coil (Signa; GE Healthcare, Milwaukee, Wis). The right hip was examined in eight patients and the left hip was examined in seven. The volunteers were randomly assigned for imaging at the right hip in five volunteers and at the left hip in four.

During MR imaging, the volunteers and patients were supine with the hip in a neutral position on a custom-made loading apparatus consisting of a back board and a sliding foot plate on low-friction rollers (Fig 1). Under the loaded condition, axial compression force was transmitted to the hip joint cranially by means of the foot plate, which was connected to a water-filled weight.

The correlation between the water volume in the tanks and the actual force applied to the foot with the foot plate was confirmed in a preliminary examination: When seven different amounts of water volume, set up evenly over a range of 15–45 kg, were examined, there was a high correlation between the water volume and the actual force applied to the foot plate, which was measured by using a spring balance ($r = 0.998$, $P < .0001$). Under the loaded condition, an axial compression force was transmitted to the hip joint by applying 50% of the body weight only to the examined leg, assuming that this would simulate loading conditions in the static standing position.

Coronal T2 maps were obtained under the loaded and unloaded conditions from two-dimensional dual-spin-echo images with the following parameters: repetition time msec/echo time msec, 1500/10 and 45; field of view, 16 cm; matrix, 512 × 256 interpolated to 512 × 512 with a resulting in-plane pixel resolution of 312.5 μm; section thickness, 5 mm; and two signals acquired for a total imaging time of 13.5 minutes. Coronal T2 maps from two-dimensional multiple-spin-echo images (repetition time, 1500 msec; eight evenly spaced echoes between 11 and 88 msec; field of

Figure 1

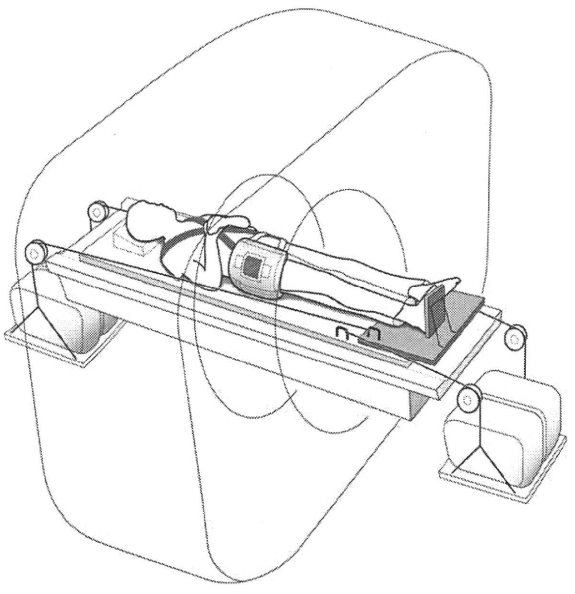

Figure 1: Schematic of the custom-made loading apparatus used during MR imaging. The foot of the examined leg was secured in a neutral rotational position by strapping it tightly to a sliding foot rest plate. The subject's shoulders were strapped tightly to the back board. Under the loading condition, axial compression force was transmitted to the hip joint cranially by means of the foot plate, which was connected to a water-filled weight. The same magnitude of counterforce was also applied to the back board caudally to prevent cranial displacement of the body.

view, 16 cm; matrix, 384 × 256; section thickness, 5 mm; two signals acquired; total imaging time, 13 minutes) were also obtained under the unloaded condition. Owing to inferior in-plane resolution, however, the coronal T2 maps from multiple-spin-echo images were used only to examine the correlation of measured T2 values with those from dual-spin-echo images. A frequency-selective fat-suppression technique was used to minimize the chemical shift artifact at the cartilage-bone interface. Frequency encoding was oriented in the cranial-to-caudal direction. First, MR images were obtained with the dual-spin-echo sequence and the multiple-spin-echo sequence under the unloaded condition by using the same axial localizing images. Then, the load was applied for an average of 6 minutes (range, 5–7 minutes), after which MR images were obtained with the dual-spin-echo sequence under the continuously loaded condition. The imaging planes were co-registered by comparing the positions on axial localizing images and coronal trial images under the loaded and unloaded conditions.

MR Imaging Data Analysis

All analyses were performed with use of the coronal images through the center of the femoral head by using custom-developed software (Baum, version 1.00; Osaka University, Osaka, Japan). The T2 value was calculated on a pixel-by-pixel basis by fitting the echo time data and corresponding signal intensity to a monoexponential equation. In the calculation of T2 values from the multiple-spin-echo images, the first echo was excluded to minimize T2 inaccuracy due to stimulated echoes (32,33). The acetabular and femoral cartilages at weight bearing were manually defined on the image corresponding to the first echo from the lateral border of the acetabular fossa to the lateral margin of the acetabulum (Fig 2). Attention was paid not to include joint fluid with high signal intensity at the surface of the acetabular and femoral cartilages on the image with the second or later echo time. Each acetabular and femoral cartilage was automatically divided into three radial sections with equal widths

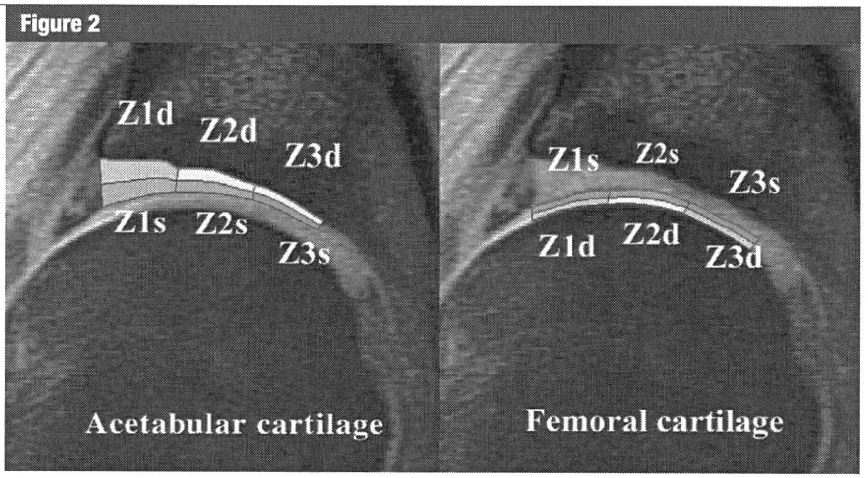

Figure 2: Images illustrate the ROIs at the weight-bearing area in the acetabular cartilage and femoral cartilage. Femoral cartilage zones Z3d and Z3s were excluded from analysis because of the frequent involvement of the ligamentum teres at the insertion to the femoral head in patients with hip dysplasia.

(zones Z1, Z2, and Z3), and each section was further divided into deep layers (zones Z1d, Z2d, and Z3d) and superficial layers (zones Z1s, Z2s, and Z3s) with equal thickness. Zones Z3d and Z3s of the femoral cartilage were excluded from analysis because of the frequent involvement of the ligamentum teres at the insertion into the femoral head in dysplastic hips. The average T2 value of each subdivided region of interest (ROI) (zones Z1s, Z1d, Z2s, Z2d, Z3s, and Z3d) and the average cartilage thickness of each ROI (zones Z1, Z2, Z3) were calculated. ROIs were measured three times, and the average T2 value and cartilage thickness were determined by one observer (T.N., with more than 10 years of experience in the study of articular cartilage imaging), who was blinded to the radiologic assessments.

Reliability of T2 measurements from dual-spin-echo images.—To assess reliability in the calculation of T2 values from dual-spin-echo images that were used in the subsequent analysis, the relationships between T2 values from dual-spin-echo images and T2 values from multiple-spin-echo images at each zone under the unloaded condition were evaluated by using the Spearman correlation coefficient.

Reproducibility of T2 and cartilage thickness measurements.—To assess the reproducibility of measurements, an additional observer (T.S., with 3 years of experience in articular cartilage imaging), who was blinded to the radiologic assessments, independently evaluated cartilage T2 and cartilage thickness from dual-spin-echo MR images under unloaded conditions in 10 subjects—the first five volunteers and the first five patients. The interobserver reproducibility in cartilage T2 and thickness at each ROI was calculated from the measurements by the two observers (T.N. and T.S.) as the coefficient of variation (expressed as percentage: [standard deviation/mean] × 100), and the mean reproducibility was calculated as the root-mean-square average of the 10 cases.

Statistical Analysis

Statistical analysis was performed by one observer (H.T., with 10 years of experience in the study of radiology) by using standard software (SPSS, version 11; SPSS, Chicago, Ill). Descriptive analysis was performed to evaluate the WOMAC pain scores, the reliability of T2 measurements with dual-spin-echo images versus that with multiple-spin-echo images, and the reproducibility of measurements between the two observers. Cartilage T2 values and cartilage thickness at each ROI under the unloaded and loaded conditions were compared between the volunteers and patients by using the nonparametric Mann-Whitney *U* test. In both volunteers and patients, cartilage T2 values and cartilage

Table 1

Relationships between Dual-Spin-Echo and Multiple-Spin-Echo T2 at Each Acetabular and Femoral Cartilage Zone

Zone	T2 with Two Echoes (msec)*	T2 with Multiple Echoes (msec)*	*r* Value	*P* Value
Acetabular cartilage				
Z1d	23.9 ± 3.4	35.4 ± 4.8	0.72	.0005
Z1s	33.7 ± 4.6	43.7 ± 6.1	0.83	.0001
Z2d	23.5 ± 3.7	34.7 ± 5.0	0.74	.0004
Z2s	34.2 ± 4.0	45.1 ± 6.0	0.78	.0002
Z3d	26.5 ± 6.2	42.1 ± 7.9	0.78	.0002
Z3s	37.9 ± 6.1	51.4 ± 9.0	0.85	.0001
Femoral cartilage				
Z1d	26.2 ± 3.3	32.7 ± 4.4	0.62	.0028
Z1s	36.1 ± 4.0	44.1 ± 4.4	0.67	.0014
Z2d	26.1 ± 5.3	33.0 ± 3.9	0.60	.0038
Z2s	35.5 ± 5.3	43.8 ± 7.2	0.82	.0001

* Data are given as means ± standard deviations.

thickness under the unloaded condition were compared with those under the loaded condition by using the Wilcoxon signed rank test. Changes in T2 values and cartilage thickness at each ROI with loading were compared between the volunteers and patients by using the nonparametric Mann-Whitney *U* test. Among the patients, the relationships between the changes in T2 with loading and age, body mass index, and center-edge angle on radiographs were evaluated by using the Spearman correlation coefficient. A *P* value of less than .05 was indicative of statistical significance.

Results

At MR imaging, a WOMAC pain score of 0 was determined in all hips of the healthy volunteers; the average WOMAC pain score of the dysplastic hips was 3.5 (range, 0–9).

Compared with T2 values from multiple-spin-echo images, T2 values from dual-spin-echo images at the corresponding zone showed lower mean values under the unloaded condition (Table 1). Results of Spearman correlation coefficient analysis showed significant correlations between both T2 values at all zones, with *r* values of 0.60–0.85.

The interobserver reproducibility of T2 measurements in the acetabular cartilage was as follows: Z1d, 2.2%; Z1s, 2.3%; Z2d, 2.6%; Z2s, 1.2%; Z3d, 5.8%; and Z3s, 3.8%. The interobserver reproducibility of T2 measurements in the femoral cartilage was as follows: Z1d, 4.5%; Z1s, 2.3%; Z2d, 4.7%; and Z2s, 1.3%. The interobserver reproducibility of cartilage thickness measurements in the acetabular cartilage was as follows: Z1, 4.9%; Z2, 5.7%; and Z3, 6.5%. The interobserver reproducibility of cartilage thickness measurements in the femoral cartilage was 6.1% for Z1 and 6.6% for Z2.

Cartilage T2 under the unloaded condition did not show a predominant trend of differences between normal and dysplastic hips (Table 2). At zone Z1d of the acetabular cartilage, T2 values of the patients were significantly greater than those of the volunteers ($P = .01$). Conversely, at zone Z1d of the femoral cartilage, T2 values of the patients were significantly lower than those of the volunteers ($P = .03$).

In volunteers, there was no significant difference between T2 values under the unloaded condition and T2 values under the loaded condition at each ROI. In patients, T2 values with loading decreased significantly at acetabular cartilage zones Z1s and Z2s ($P = .02$ and $P = .04$, respectively). At acetabular cartilage zone Z1s, the decrease in T2 values with loading was significantly greater in patients with dysplasia than in healthy volunteers ($P = .04$) (Table 2, Figs 3, 4).

With respect to cartilage thickness, the cartilage at most zones of the acetabular and femoral cartilage in dysplastic hips was significantly thicker than that in normal hips (Table 3). In volunteers, there was no significant difference between cartilage thickness under the unloaded condition and cartilage thickness under the loaded condition at each ROI. In patients, cartilage thickness with loading decreased significantly at acetabular cartilage zone Z1 ($P = .02$). However, there were no significant differences in the changes in cartilage thickness between the volunteers and patients.

Among patients with hip dysplasia, results of Spearman correlation coefficient analysis showed an inverse correlation between patient age and T2 changes with loading at acetabular cartilage zone Z2d ($P = .04$, $r = -0.52$, Fig 5a) and at femoral cartilage zone Z1d ($P = .03$, $r = -0.60$, Fig 5b). Moreover, there was a positive correlation between center-edge angle and T2 changes with loading at acetabular cartilage zone Z1d ($P = .03$, $r = 0.67$, Fig 5c). There was no significant correlation between the T2 changes with loading and the body mass index of the patients at each ROI.

Discussion

Normal hip joint biomechanics relating to pressure distribution on the articular cartilage and acetabular labrum have been studied extensively by using cadavers and computational-mathematical modeling (2,4,16,34,35). Konrath et al (34) measured the contact pressure between the acetabulum and femoral head of cadaveric hips by using a pressure-sensitive film and showed a tendency for a peripheral increase in load with maximal strength at the superior region of the normal acetabulum in a simulated single-limb stance. By using a computational simplified hip model, Chegini et al (16) showed an inverse correlation between the center-edge angle and the peak contact pressure with focal overloading of the lateral edge of the

Table 2

T2 Value under Unloaded and Loaded Conditions and T2 Changes with Loading at Each Acetabular and Femoral Cartilage Zone

	T2 without Loading (msec)			T2 with Loading (msec)			T2 Change with Loading (%)†		
Zone	Volunteers*	Patients*	*P* Value	Volunteers*	Patients*	*P* Value	Volunteers*	Patients*	*P* Value
Acetabular cartilage									
Z1d	21.6 ± 2.7	25.4 ± 3.1	.01‡	23.4 ± 4.1	25.2 ± 4.6	.40	8.7 ± 14.6	−0.7 ± 11.5	.07
Z1s	32.8 ± 3.0	34.2 ± 5.4	.53	33.0 ± 3.0	31.6 ± 6.2	.53	1.2 ± 10.9	−7.6 ± 10.6	.04‡
Z2d	21.7 ± 3.0	24.5 ± 3.8	.13	22.1 ± 3.6	25.5 ± 4.7	.11	1.6 ± 6.9	4.4 ± 13.3	.46
Z2s	33.3 ± 4.1	34.7 ± 4.0	.42	32.1 ± 3.3	33.3 ± 3.3	.39	−3.2 ± 7.2	−3.6 ± 6.7	.93
Z3d	27.7 ± 6.9	25.8 ± 5.9	.57	28.1 ± 7.2	25.9 ± 5.4	.42	4.4 ± 26.9	1.2 ± 13.9	.98
Z3s	39.8 ± 5.1	36.7 ± 6.4	.22	39.0 ± 5.7	34.4 ± 4.8	.04‡	−1.3 ± 14.4	−4.6 ± 14.8	.53
Femoral cartilage									
Z1d	28.3 ± 3.5	25.0 ± 2.6	.03‡	27.0 ± 3.7	26.6 ± 3.9	.70	−4.0 ± 11.9	6.5 ± 13.5	.06
Z1s	36.1 ± 3.5	36.1 ± 4.3	.74	36.7 ± 4.9	34.6 ± 4.4	.39	1.9 ± 10.8	−3.6 ± 12.6	.33
Z2d	23.1 ± 4.5	27.8 ± 5.1	.06	22.3 ± 3.0	27.9 ± 3.4	.001‡	−1.9 ± 13.7	2.1 ± 15.0	.70
Z2s	34.1 ± 4.9	36.4 ± 5.5	.13	33.6 ± 4.9	34.6 ± 5.7	.57	−1.0 ± 9.1	−4.5 ± 9.8	.39

* Data are given as means ± standard deviations.

† T2 change with loading was calculated for each volunteer or patient as follows: [(T2 value with loading − T2 value without loading)/T2 value without loading] × 100.

‡ The difference between the two groups was statistically significant.

acetabulum in dysplastic hips during simulated walking. There are large individual variations in the three-dimensional morphologic and material properties of the articular cartilage among patients with hip dysplasia (36). To our knowledge, there has been no biomechanical patient-specific analysis of patients with hip dysplasia reflecting morphologic and material diversions of the articular cartilage of individual patients.

MR imaging has the potential to help evaluate the load responsiveness of an articular cartilage. Rubenstein et al (17) observed a gradual decrease in the signal intensity of an excised bovine cartilage, beginning at the superficial cartilage layers and progressing to the overall depth of the cartilage with increasing pressure. A decrease in MR signal intensity with loading can be explained by extrusion of interstitial water and deformation of cartilage architecture within the cartilage (17,19). With use of high-spatial-resolution microscopic MR imaging, Alhadlaq and Xia (18) studied T2 changes in beagle cartilage specimens in response to external loading and found that the change in cartilage T2 showed a positive correlation with the strain value of compression.

Figure 3

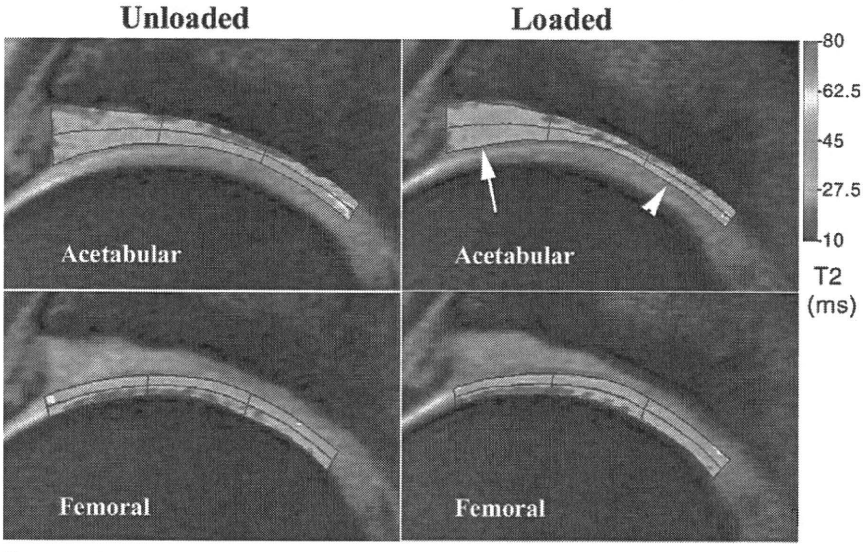

Figure 3: T2 maps of the acetabular and femoral cartilage on midcoronal MR images in a 30-year-old female volunteer. A low T2 is indicated by blue, and a high T2 is indicated by green or red. Under the loaded condition, the T2 of the acetabular cartilage was increased at the outer zones (Z1s and Z1d, arrow) and decreased at the inner, superficial zone (Z3s, arrowhead).

In the present study, we evaluated the change in cartilage T2 in the hip joint of living human subjects with loading. The topographic variation of cartilage T2, with higher T2 values at superficial zones in unloaded conditions, agrees with findings from a previous clinical study (37). The average T2 values with loading decreased at most superficial zones of the acetabular and femoral cartilages. This

Table 3

Cartilage Thickness under Unloaded and Loaded Conditions and Changes in Thickness with Loading at Each Acetabular and Femoral Cartilage Zone

	Thickness without Loading (mm)			Thickness with Loading (mm)			Change in Thickness with Loading (%)†		
Zone	Volunteers*	Patients*	*P* Value	Volunteers*	Patients*	*P* Value	Volunteers*	Patients*	*P* Value
Acetabular cartilage									
Z1	2.1 ± 0.7	2.4 ± 0.5	.08	2.2 ± 0.7	2.2 ± 0.6	.49	3.4 ± 12.9	−7.9 ± 11.5	.08
Z2	1.6 ± 0.3	2.2 ± 0.5	.001‡	1.6 ± 0.4	2.2 ± 0.4	.004‡	−2.6 ± 9.5	−1.8 ± 9.4	.74
Z3	1.5 ± 0.3	1.9 ± 0.4	.018‡	1.5 ± 0.2	1.9 ± 0.4	.001‡	−2.2 ± 14.0	2.6 ± 8.9	.32
Femoral cartilage									
Z1	1.2 ± 0.2	1.6 ± 0.3	.001‡	1.2 ± 0.2	1.7 ± 0.4	.008‡	4.5 ± 17.6	2.8 ± 15.8	.61
Z2	1.2 ± 0.2	1.8 ± 0.4	.001‡	1.2 ± 0.3	1.8 ± 0.4	.001‡	−0.8 ± 15.2	−0.4 ± 14.5	.74

* Data are given as means ± standard deviations.

† Changes were calculated for each volunteer or patient as follows: (cartilage thickness with loading − cartilage thickness without loading)/cartilage thickness without loading × 100.

‡ The difference between the two groups was statistically significant.

Figure 4

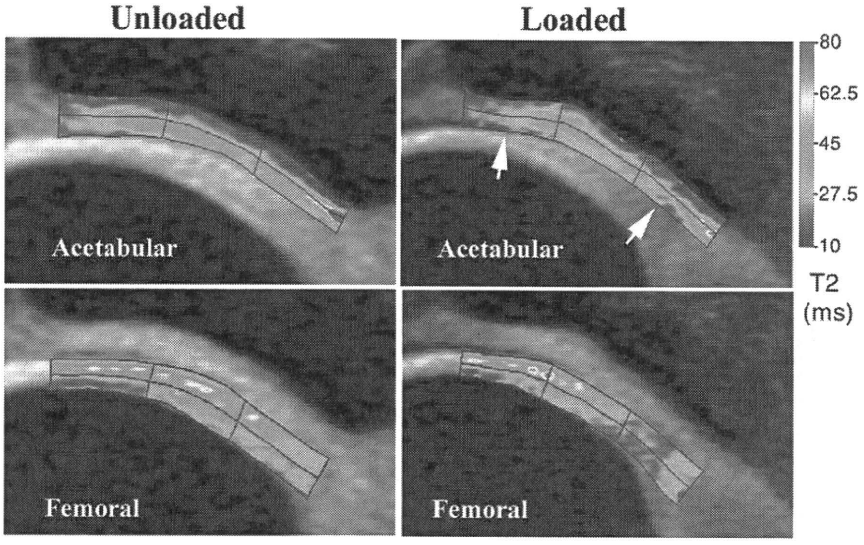

Figure 4: T2 maps of the acetabular and femoral cartilage on midcoronal MR images in a 28-year-old woman with hip dysplasia. Under the loaded condition, the T2 of the acetabular cartilage was decreased at both the outer and inner superficial zones (Z1s and Z3s, respectively, arrows).

finding was consistent with those from previous experimental studies (17,18). Although the mode of loading was different from that used in the present study, results of a clinical investigation evaluating cartilage T2 response to high-impact exercise with a cyclic compressive load showed a significant decrease in T2 values in the superficial femoral cartilage in the knee joints of healthy volunteers after 30 minutes of running (32). More important, we found that the decrease in T2 values at the outer superficial acetabular cartilage area with loading was significantly greater in dysplastic hips than in normal hips. Assuming that the decrease in T2 reflects changes in the solid matrix of the cartilage or interstitial water, our findings may indicate that dysplastic hips were subject to a substantial alteration in the extracellular matrix composition and/or fluid distribution at the outer acetabular cartilage when a load was applied.

Two underlying pathomechanisms may help explain this response. First, a decrease in T2 with loading might reflect a concentrated load-bearing force at the outer acetabular cartilage in dysplastic hips. This is supported by results of previous computational studies in which hip joint contact pressure was estimated (4,16) and the correlation between center-edge angle and T2 decrease with loading in our study. Second, a large T2 decrease in dysplastic hips with loading might indicate that the outer area of the acetabular cartilage was already involved in degenerative changes or injury and failed to appropriately adapt to the external compression force due to increased hydration and disorganized collagen structure within the cartilage. This assumption was partly supported by a significant increase in T2 at the outer acetabular cartilage in dysplastic hips, presumably in association with degenerative changes in the cartilage (38,39). Regardless of the possible mechanism, cartilage T2 mapping with loading presumably enabled the detection of a mechanically critical cartilage area where substantial changes in the ultrastructure or molecular composition of the cartilage occurred when a physiologic load was applied.

Patient age was inversely correlated with T2 changes at the deep zones of the acetabular and femoral cartilage

Figure 5

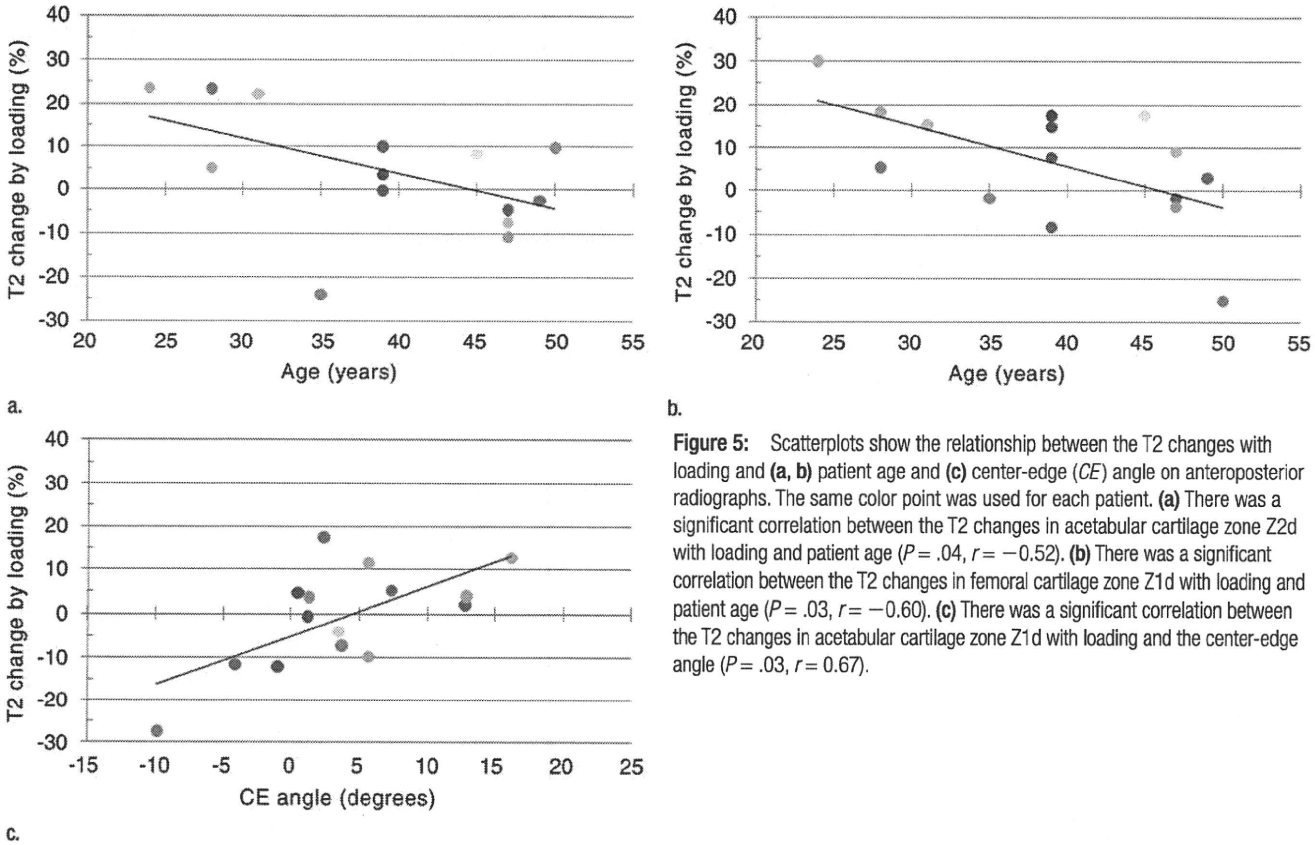

Figure 5: Scatterplots show the relationship between the T2 changes with loading and **(a, b)** patient age and **(c)** center-edge (*CE*) angle on anteroposterior radiographs. The same color point was used for each patient. **(a)** There was a significant correlation between the T2 changes in acetabular cartilage zone Z2d with loading and patient age ($P = .04$, $r = -0.52$). **(b)** There was a significant correlation between the T2 changes in femoral cartilage zone Z1d with loading and patient age ($P = .03$, $r = -0.60$). **(c)** There was a significant correlation between the T2 changes in acetabular cartilage zone Z1d with loading and the center-edge angle ($P = .03$, $r = 0.67$).

with loading. A previous experimental study in which compression force was applied on bone-cartilage plugs (17) showed a decrease of MR signal intensity in the superficial zone along with an increase of signal intensity in the deep zone at an initial pressure. These signal intensity changes were mainly accounted for by the depth-dependent movement of water content and deformation of the collagen architecture within the cartilage: With loading, interstitial water exudes from the cartilage surface or moves to a deeper zone of the cartilage, and this may contribute to the decrease of T2 in the superficial zone and the increase of T2 in the deep zone. With loading, originally parallel collagen fibers aligned perpendicular to the subchondral plate in the deep zone spread out and the portion of fibers oriented at the magic angle with respect to the static magnetic field increases; this may lead to an increase of cartilage T2 in the deep zone (40). With aging, however, permeability to fluid flow in the cartilage decreases (41) or cartilage stiffness increases in association with the accumulation of nonenzymatic glycation products (42), which may cause a depth-wise variation in T2 change with loading between younger and older patients.

T2 values calculated from two echoes were used for the evaluation of load responsiveness in cartilage T2. In many previous studies, T2 was calculated from images obtained with more than two echoes, and the initial echo image obtained with multiple-spin-echo imaging was excluded in the calculation of T2 to minimize T2 inaccuracy caused by stimulated echoes (32,33); however, the multiple-spin-echo sequence available in this study provided inferior image quality with lower in-plane resolution. A previous study in which a dual-spin-echo sequence was used for T2 assessment successfully achieved significant differences between the knee cartilages of healthy subjects and patients with osteoarthritis (38). Given the sufficiently high correlation to T2 values from multiple-spin-echo images in the present study, we consider T2 assessment with a dual-spin-echo sequence to provide a reliable assessment of the extracellular matrix in the hip cartilage. Although the present image acquisition sequence was not optimized for measuring cartilage thickness, most zones of the acetabular and femoral cartilage were significantly thicker in patients with dysplasia than in healthy volunteers. This finding was consistent with that from a previous study that used MR imaging with fat-suppressed three-dimensional fast spoiled gradient-echo sequences (43). In our study, however, evaluation of cartilage thickness with loading did not enable the detection of a difference in response to loading between healthy volunteers and patients with hip dysplasia.

MR imaging under the loaded condition was examined previously in patients with an upright posture in the evaluation of the cartilage contact area in the knee or impingement between the femoral neck and the acetabular rim in the hip by using open-configuration MR units (44,45). The image quality obtained with open-configuration MR units is relatively low owing to the low magnetic field strength (0.5 T), and MR images obtained with patients in an upright position are more susceptible to motion artifacts. We assumed that the use of a closed-bore MR unit with a high field strength (3.0 T) and the application of a mechanical loading device with the patient in a supine posture were suitable for assessing cartilage microstructural properties with loading because a high image resolution can be acquired with a sufficient signal-to-noise ratio. In a previous investigation in which a similar mechanical device was used, compressive loading at T2 mapping of knee cartilage was successfully evaluated (46). However, it is unclear how accurately this system simulated the mechanical environment in the physiologic standing position because it did not incorporate surrounding muscle action such as contraction of the iliopsoas, gluteus maximus, and gluteus medius muscles and the relative angular and rotational position of the pelvis against the femoral head might be different.

This study had several limitations. First, cartilage T2 was assessed only on midcoronal hip joint images, and anterior or posterior areas of the acetabular and femoral cartilage were not evaluated because the extensively curved joint surface is susceptible to partial volume averaging. Additional investigations with various imaging planes are necessary to clarify load responsiveness over the entire articular cartilage. Second, delineation of the cartilage surface in ROI placement may be difficult owing to the close contact between the acetabular and femoral cartilages—particularly under the loaded condition. Furthermore, T2 assessment of most superficial cartilage areas is also susceptible to partial volume averaging with synovial fluid on the midcoronal images, and this might be accentuated with the use of relatively thick sections (5 mm). By referring to the corresponding images obtained with a longer echo time, we were careful not to include joint fluid in the ROIs. However, to diminish these inherent difficulties in delineating the cartilage surface and to decrease the susceptibility of the hip joint to partial volume artifacts, further improvement is necessary so that images can be acquired with a higher spatial resolution and a sufficient signal-to-noise ratio. Third, dysplastic hips at both the prearthritic and early arthritic stage were examined in this study. Because hips with radiologic findings of osteoarthritis have a high incidence of cartilage abnormalities (39,47), the responsiveness of cartilage T2 to loading may be partly influenced by the underlying cartilage degeneration in hip dysplasia. Because of the small number of patients in this study, the load responsiveness of cartilage T2 was not compared between patients at a prearthritic stage and those at an early arthritic stage, and further investigations with a larger number of patients are needed to explore the influence of the radiologic osteoarthritis stage on the response of cartilage T2 to loading. Fourth, the response of cartilage thickness and T2 to loading was evaluated after preloading for an average of 6 minutes, followed by loading for 13.5 minutes during MR imaging. Herberhold et al (48) studied the deformational behavior of the articular cartilage during static loading of 150% of the body weight with femoropatellar knee imaging ex vivo; the deformations of the patellar and femoral cartilages after 8 minutes of compression were 25%–30% of the final deformations of those cartilages after 214 minutes of compression. It was unknown whether deformational equilibrium of the articular cartilage was achieved after preloading for an average of 6 minutes in this study. Although the location of the cartilage and magnitude of compression force used in our study differed from those used by Herberhold et al (48), our results may represent a relatively early response of the hip cartilage under static loading, simulating the status of the articular cartilage in the standing position for a relatively short period. In addition, the numbers of volunteers and patients were small. Because this was, to our knowledge, the first investigation to compare loaded cartilage T2 mapping in patients with hip dysplasia and healthy volunteers, we were not able to perform power analysis for a sufficient number of subjects before the start of the study. However, because we observed a significant difference in the T2 response of cartilage to loading between the patients and volunteers, we believe that loaded cartilage T2 mapping may help detect mechanically critical cartilage areas in patients with hip dysplasia. The volunteers were significantly younger than the patients. Previous reports have indicated that the T2 of the knee joint is significantly affected by age (33). Although the relationship between age and the T2 of cartilage in the hip joint was not clarified, the significant differences in T2 with unloading and T2 changes with loading between the volunteers and patients could have been partly influenced by the relatively large age difference between the groups. Additional studies are required to compare the response of cartilage T2 to loading between age-matched volunteers and patients.

In conclusion, the decrease of cartilage T2 at the outer superficial zones of the acetabular cartilage with loading was significantly greater in patients with hip dysplasia than in healthy volunteers. This site-specific change in cartilage T2 with loading presumably represents a mechanically critical response in which substantial changes occur in the ultrastructure or molecular composition of the cartilage. Additional follow-up studies are needed to clarify the potential of using T2 changes with loading to predict the subsequent progression of osteoarthritis.

References

1. Harris WH. Etiology of osteoarthritis of the hip. Clin Orthop Relat Res 1986;(213):20–33.

2. Michaeli DA, Murphy SB, Hipp JA. Comparison of predicted and measured contact pressures in normal and dysplastic hips. Med Eng Phys 1997;19(2):180–186.

3. Hadley NA, Brown TD, Weinstein SL. The effects of contact pressure elevations and aseptic necrosis on the long-term outcome of congenital hip dislocation. J Orthop Res 1990;8(4):504–513.

4. Hipp JA, Sugano N, Millis MB, Murphy SB. Planning acetabular redirection osteotomies based on joint contact pressures. Clin Orthop Relat Res 1999;(364):134–143.

5. Genda E, Iwasaki N, Li G, MacWilliams BA, Barrance PJ, Chao EY. Normal hip joint contact pressure distribution in single-leg standing: effect of gender and anatomic parameters. J Biomech 2001;34(7):895–905.

6. Anwar MM, Sugano N, Matsui M, Takaoka K, Ono K. Dome osteotomy of the pelvis for osteoarthritis secondary to hip dysplasia: an over five-year follow-up study. J Bone Joint Surg Br 1993;75(2):222–227.

7. Zhang W, Moskowitz RW, Nuki G, et al. OARSI recommendations for the management of hip and knee osteoarthritis. II. OARSI evidence-based, expert consensus guidelines. Osteoarthritis Cartilage 2008;16(2):137–162.

8. Lane NE, Lin P, Christiansen L, et al. Association of mild acetabular dysplasia with an increased risk of incident hip osteoarthritis in elderly white women: the study of osteoporotic fractures. Arthritis Rheum 2000;43(2):400–404.

9. Reijman M, Hazes JM, Pols HA, Koes BW, Bierma-Zeinstra SM. Acetabular dysplasia predicts incident osteoarthritis of the hip: the Rotterdam study. Arthritis Rheum 2005;52(3):787–793.

10. Delaunay S, Dussault RG, Kaplan PA, Alford BA. Radiographic measurements of dysplastic adult hips. Skeletal Radiol 1997;26(2):75–81.

11. Day WH, Swanson SA, Freeman MA. Contact pressures in the loaded human cadaver hip. J Bone Joint Surg Br 1975;57(3):302–313.

12. Genda E, Konishi N, Hasegawa Y, Miura T. A computer simulation study of normal and abnormal hip joint contact pressure. Arch Orthop Trauma Surg 1995;114(4):202–206.

13. Ferguson SJ, Bryant JT, Ganz R, Ito K. The influence of the acetabular labrum on hip joint cartilage consolidation: a poroelastic finite element model. J Biomech 2000;33(8):953–960.

14. Rapperport DJ, Carter DR, Schurman DJ. Contact finite element stress analysis of the hip joint. J Orthop Res 1985;3(4):435–446.

15. Wang Y, Wei HW, Yu TC, Cheng CK. Parametric analysis of the stress distribution on the articular cartilage and subchondral bone. Biomed Mater Eng 2007;17(4):241–247.

16. Chegini S, Beck M, Ferguson SJ. The effects of impingement and dysplasia on stress distributions in the hip joint during sitting and walking: a finite element analysis. J Orthop Res 2009;27(2):195–201.

17. Rubenstein JD, Kim JK, Henkelman RM. Effects of compression and recovery on bovine articular cartilage: appearance on MR images. Radiology 1996;201(3):843–850.

18. Alhadlaq HA, Xia Y. The structural adaptations in compressed articular cartilage by microscopic MRI (microMRI) T(2) anisotropy. Osteoarthritis Cartilage 2004;12(11):887–894.

19. Liess C, Lüsse S, Karger N, Heller M, Glüer CC. Detection of changes in cartilage water content using MRI T2-mapping in vivo. Osteoarthritis Cartilage 2002;10(12):907–913.

20. Burstein D, Gray ML. Is MRI fulfilling its promise for molecular imaging of cartilage in arthritis? Osteoarthritis Cartilage 2006;14(11):1087–1090.

21. Link TM, Stahl R, Woertler K. Cartilage imaging: motivation, techniques, current and future significance. Eur Radiol 2007;17(5):1135–1146.

22. Eckstein F, Burstein D, Link TM. Quantitative MRI of cartilage and bone: degenerative changes in osteoarthritis. NMR Biomed 2006;19(7):822–854.

23. Nieminen MT, Töyräs J, Rieppo J, et al. Quantitative MR microscopy of enzymatically degraded articular cartilage. Magn Reson Med 2000;43(5):676–681.

24. Lüsse S, Claassen H, Gehrke T, et al. Evaluation of water content by spatially resolved transverse relaxation times of human articular cartilage. Magn Reson Imaging 2000;18(4):423–430.

25. Inoue K, Wicart P, Kawasaki T, et al. Prevalence of hip osteoarthritis and acetabular dysplasia in French and Japanese adults. Rheumatology (Oxford) 2000;39(7):745–748.

26. Mosher TJ, Collins CM, Smith HE, et al. Effect of gender on in vivo cartilage magnetic resonance imaging T2 mapping. J Magn Reson Imaging 2004;19(3):323–328.

27. Fredensborg N. The CE angle of normal hips. Acta Orthop Scand 1976;47(4):403–405.

28. Crowe JF, Mani VJ, Ranawat CS. Total hip replacement in congenital dislocation and dysplasia of the hip. J Bone Joint Surg Am 1979;61(1):15–23.

29. Kellgren JH, Lawrence JS. Radiological assessment of osteo-arthrosis. Ann Rheum Dis 1957;16(4):494–502.

30. Reijman M, Hazes JM, Pols HA, Bernsen RM, Koes BW, Bierma-Zeinstra SM. Validity and reliability of three definitions of hip osteoarthritis: cross sectional and longitudinal approach. Ann Rheum Dis 2004;63(11):1427–1433.

31. Bellamy N, Buchanan WW, Goldsmith CH, Campbell J, Stitt LW. Validation study of WOMAC: a health status instrument for measuring clinically important patient relevant outcomes to antirheumatic drug therapy in patients with osteoarthritis of the hip or knee. J Rheumatol 1988;15(12):1833–1840.

32. Mosher TJ, Smith HE, Collins C, et al. Change in knee cartilage T2 at MR imaging after running: a feasibility study. Radiology 2005;234(1):245–249.

33. Mosher TJ, Dardzinski BJ, Smith MB. Human articular cartilage: influence of aging and early symptomatic degeneration on the spatial variation of T2—preliminary findings at 3 T. Radiology 2000;214(1):259–266.

34. Konrath GA, Hamel AJ, Olson SA, Bay B, Sharkey NA. The role of the acetabular labrum and the transverse acetabular ligament in load transmission in the hip. J Bone Joint Surg Am 1998;80(12):1781–1788.

35. von Eisenhart R, Adam C, Steinlechner M, Müller-Gerbl M, Eckstein F. Quantitative determination of joint incongruity and pressure distribution during simulated gait and cartilage thickness in the human hip joint. J Orthop Res 1999;17(4):532–539.

36. Noble PC, Kamaric E, Sugano N, et al. Three-dimensional shape of the dysplastic femur: implications for THR. Clin Orthop Relat Res 2003;(417):27–40.

37. Watanabe A, Boesch C, Siebenrock K, Obata T, Anderson SE. T2 mapping of hip articular cartilage in healthy volunteers at 3T: a study of topographic variation. J Magn Reson Imaging 2007;26(1):165–171.

38. Dunn TC, Lu Y, Jin H, Ries MD, Majumdar S. T2 relaxation time of cartilage at MR imaging: comparison with severity of knee osteoarthritis. Radiology 2004;232(2):592–598.

39. Nishii T, Tanaka H, Sugano N, Sakai T, Hananouchi T, Yoshikawa H. Evaluation of cartilage matrix disorders by T2 relaxation time in patients with hip dysplasia. Osteoarthritis Cartilage 2008;16(2):227–233.

40. Gründer W, Kanowski M, Wagner M, Werner A. Visualization of pressure distribution within loaded joint cartilage by application of angle-sensitive NMR microscopy. Magn Reson Med 2000;43(6):884–891.

41. Grushko G, Schneiderman R, Maroudas A. Some biochemical and biophysical parameters for the study of the pathogenesis of osteoarthritis: a comparison between the processes of ageing and degeneration in human hip cartilage. Connect Tissue Res 1989;19(2-4):149–176.

42. Bank RA, Bayliss MT, Lafeber FP, Maroudas A, Tekoppele JM. Ageing and zonal variation in post-translational modification of collagen in normal human articular cartilage: the age-related increase in non-enzymatic glycation affects biomechanical properties of cartilage. Biochem J 1998; 330(pt 1):345–351.

43. Nishii T, Sugano N, Sato Y, Tanaka H, Miki H, Yoshikawa H. Three-dimensional distribution of acetabular cartilage thickness in patients with hip dysplasia: a fully automated computational analysis of MR imaging. Osteoarthritis Cartilage 2004;12(8):650–657.

44. Gold GE, Besier TF, Draper CE, Asakawa DS, Delp SL, Beaupre GS. Weight-bearing MRI of patellofemoral joint cartilage contact area. J Magn Reson Imaging 2004;20(3):526–530.

45. Yamamura M, Miki H, Nakamura N, Murai M, Yoshikawa H, Sugano N. Open-acetabular impingement. J Orthop Res 2007;25(12): 1582–1588.

46. Nishii T, Kuroda K, Matsuoka Y, Sahara T, Yoshikawa H. Change in knee cartilage T2 in response to mechanical loading. J Magn Reson Imaging 2008;28(1):175–180.

47. Noguchi Y, Miura H, Takasugi S, Iwamoto Y. Cartilage and labrum degeneration in the dysplastic hip generally originates in the anterosuperior weight-bearing area: an arthroscopic observation. Arthroscopy 1999;15(5):496–506.

48. Herberhold C, Faber S, Stammberger T, et al. In situ measurement of articular cartilage deformation in intact femoropatellar joints under static loading. J Biomech 1999;32(12):1287–1295.

Osteoarthritis and Cartilage 18 (2010) 902–908

Osteoarthritis and Cartilage

Loading and knee alignment have significant influence on cartilage MRI T2 in porcine knee joints

T. Shiomi †, T. Nishii †‡*, H. Tanaka §, Y. Yamazaki ||, K. Murase ||, A. Myoui †¶, H. Yoshikawa †, N. Sugano †‡

† Department of Orthopaedic Surgery, Osaka University Medical School, Osaka, Japan
‡ Department of Orthopaedic Medical Engineering, Osaka University Medical School, Osaka, Japan
§ Department of Radiology, Osaka University Medical School, Osaka, Japan
|| Department of Medical Physics and Engineering, Osaka University Medical School, Osaka, Japan
¶ Medical Center for Translational Research, Osaka University Hospital, Osaka, Japan

ARTICLE INFO

Article history:
Received 14 October 2009
Accepted 3 May 2010

Keywords:
MRI
Cartilage
T2
Static loading
Knee alignment

SUMMARY

Objective: Physiological magnetic resonance imaging (MRI) under loading or knee malalignment conditions has not been thoroughly investigated. We assessed the influence of static loading and knee alignment on T2 (transverse relaxation time) mapping of the knee femoral cartilage of porcine knee joints using a non-metallic pressure device.

Methods: Ten porcine knee joints were harvested *en bloc* with intact capsules and surrounding muscles and imaged using a custom-made pressure device and 3.0-T MRI system. Sagittal T2 maps were obtained (1) at knee neutral alignment without external loading (no loading), (2) under mechanical compression of 140 N (neutral loading), and (3) under the same loading conditions as in (2) with the knee at 10° varus alignment (varus loading). T2 values of deep, intermediate, and superficial zones of the medial and lateral femoral cartilages at the weight-bearing area were compared among these conditions using custom-made software. Cartilage contact pressure between the femoral and tibial cartilages, measured by a pressure-sensitive film, was correlated with cartilage T2 measurements.

Results: In the medial cartilage, mean T2 values of the deep, intermediate, and superficial zones decreased by 1.4%, 13.0%, and 6.0% under neutral loading. They further decreased by 4.3%, 19.3%, and 17.2% under varus loading compared to no loading. In the lateral cartilage, these mean T2 values decreased by 3.9%, 7.7%, and 4.2% under neutral loading, but increased by 1.6%, 9.6%, and 7.2% under varus loading. There was a significant decrease in T2 values in the intermediate zone of the medial cartilage under both neutral and varus loading, and in the superficial zone of the medial cartilage under varus loading ($P < 0.05$). Total contact pressure values under neutral loading and varus loading conditions significantly correlated with T2 values in the superficial and intermediate zones of the medial cartilages.

Conclusions: The response of T2 to change in static loading or alignment varied between the medial and lateral cartilages, and among the deep, intermediate, and superficial zones. These T2 changes were significantly related to the contact pressure measurements. Our results indicate that T2 mapping under loading allows non-invasive, biomechanical assessment of site-specific stress distribution in the cartilage.

Introduction

Knee imaging using quantitative magnetic resonance imaging (MRI) techniques such as delayed gadolinium-enhanced MRI of cartilage (dGEMRIC), transverse relaxation time (T2) mapping and T1rho showed great advancements in non-invasive assessment of the articular cartilage, particularly with regard to matrix composition and degenerative changes[1–4]. Sensitive evaluations of water, collagen, and proteoglycan content or collagen arrangement in the cartilage *in vivo* were made using the aforementioned techniques, without performing destructive retrieval analysis. Quantitative MRI revealed site-specific and age- or sex-dependent variation in normal cartilage composition and allowed early detection of osteoarthritic involvement of knee cartilages[3,5]. MRI in most of these investigations was performed without externally loading the knee with patients or volunteers lying supine on the imaging table.

The articular cartilage in the knee joint has a load-bearing function in conjunction with the interposed meniscus owing to its highly organized collagen architecture and the osmotic pressure

* Address correspondence and reprint requests to: Takashi Nishii, Department of Orthopaedic Medical Engineering, Osaka University Medical School, 2-2 Yamadaoka, Suita, Osaka 565-0871, Japan. Tel: 81-6-6879-3271; Fax: 81-6-6879-3272.
E-mail address: nishii@ort.med.osaka-u.ac.jp (T. Nishii).

1063-4584/$ – see front matter © 2010 Osteoarthritis Research Society International. Published by Elsevier Ltd. All rights reserved.
doi:10.1016/j.joca.2010.05.002

due to proteoglycan and interstitial water. While performing daily activities such as standing or walking, the articular cartilage in the knee joint is subjected to substantial external loading, which leads to cartilage deformation along with alteration in the collagen architecture or water distribution within the cartilage[6,7]. This property of the cartilage under loading differs among individuals, depending upon factors such as weight, knee alignment, ligament instability, and involvement of injury or degeneration of the cartilage and meniscus. Therefore, it is important to evaluate the articular cartilage under loading for each individual to understand the physiological and biomechanical status of the knee and to explore the disorders of stress resistance function of the cartilage that may lead to progression of osteoarthritis.

Responsiveness of the normal cartilage to compressive loading was investigated using excised cartilage plugs or exposed articular surfaces in experimental studies on MRI[8–10]. Changes in cartilage thickness and signal intensity were observed in response to an increase in loading. Among all MRI parameters, cartilage T2 mapping of cartilage is influenced by water content and collagen fiber orientation of cartilage and is indicated as a potent quantitative index for the load response of the articular cartilage[11–13]. However, few studies have investigated the load response of the articular cartilage in an intact knee joint, with preservation of the other fundamental structures such as menisci, ligaments, and capsules.

We developed a non-metallic pressure device for intact porcine knee joints that allowed MRI under variable loading or knee alignment conditions as a whole-joint model retaining the menisci, ligaments, and capsules *in situ*. The purpose of this study was to assess the load-bearing function of the femoral cartilage in association with knee alignment, using cartilage T2 as a surrogate of cartilage matrix changes.

Materials and methods

Preparation of porcine specimens and loading device

Ten fresh porcine knee joints were harvested *en bloc* with intact capsules and surrounding muscles and stored at −40°C. On the day of MRI, specimens were thawed at room temperature before the investigation. After conducting imaging and mechanical experiments, macroscopic inspection of the joint surfaces did not reveal any signs of joint disease or cartilage degeneration in the specimens used.

Knee joints were mounted in the non-metallic custom compression device, which was fitted into the head coil (eight-channel brain phased array coil, GE Healthcare, WI, USA) of an MRI scanner (Fig. 1). The femoral shaft was firmly fixed to the non-mobile base of the device by holding it between two acryl blades. The tibia was firmly fixed to the opposite side of the mobile plate such that tibial movement along the longitudinal axis and varus/valgus rotation of the knee was possible. The knee was positioned at 20° flexion, simulating the normal standing position of pigs. Under static loading conditions, axial compression force was transmitted to the knee joint *via* a sliding plate bounded by a foam material. The load was generated by a screw compression driver on one end. The viscoelastic foam material, which was made of polyolefin elastomer (Fig. 1), was compressed by 10 mm displacement and the uniaxial constitution force according to the degree of displacement was transmitted to the knee joint through an acryl plate. We used new foam material on each knee joint to avoid degeneration of the foam material. Hayashi *et al.* studied static and dynamic characteristics and stability of some kinds of elastomeric polymers by uniaxial tensile and fatigue tests in air, and demonstrated polyolefin elastomer had little stress relaxation[14]. The compression force was applied to achieve 140 N across the tibiofemoral joint, which corresponded to approximately one-third of the body weight of the specimen.

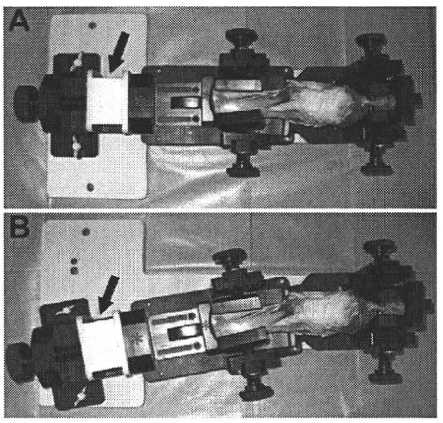

Fig. 1. Custom-made compression device along with a porcine knee joint. Axial compression force was transmitted to the knee joint *via* a sliding plate (*) bounded by a viscoelastic foam material (arrow). A: neutral position. B: 10° varus position.

Accuracy test of loading in custom compression device

In a preliminary test, loading force in the custom compression device was measured using an incompressible testing rod equipped with a load cell (TU-BR, TEAC, Japan). The accuracy of the load cell is within 0.05% rated output in non-linearity which means accuracy of linear output, and within 0.05% rated output in hysteresis which means reproducibility during loading. Compression force equivalent to 140 N was applied continuously, and real force across the testing rod was recorded from the load cell after 5, 10 and 30 min of compression to determine the time course of change in force measurements. This test was repeated five times, and the mean force measurements and the values of coefficient of variation [standard deviation/mean × 100 (%)] were 140 N and 1.5% at 5 min, 138 N and 1.5% at 10 min, and 134 N and 1.8% at 30 min. We confirmed that constant pressure was applied after 5 min–30 min of compression by the loading device.

MRI

MRI was performed using a 3.0-T MRI system (GE Healthcare). The device was placed in a head-first orientation in the center of the head coil. First, sagittal T2 maps and three-dimensional (3D) spoiled gradient-echo (SPGR) images were obtained for the lateral and medial femorotibial joints with neutral knee alignment and no external compression (no loading). Next, sagittal T2 maps and 3D SPGR images were obtained after 5 min of compression (neutral loading-1). After imaging at neutral loading-1, compression was continued for 30 min. Sagittal T2 maps and 3D SPGR images were obtained again after 30 min of compression (neutral loading-2) to examine the influence of loading duration on cartilage T2 measurements compared with neutral loading-1. Finally, sagittal T2 maps and 3D SPGR images were obtained under the same compression conditions as above with the knee at 10° varus alignment (varus loading).

T2 maps were generated using a monoexponential fit from two-dimensional (2D) multi-spin echo sequences (TR, 1500 ms; eight echoes between 10.0 ms and 80.0 ms; field of view, 10 cm; matrix, 384 × 256; slice thickness, 3 mm; signal averaging, 1; acquiring time, 6 min and 51 s). Frequency encoding was oriented in the cranial-to-caudal direction. 3D SPGR images were acquired with fat suppression (TR, 50 ms; TE, 10 ms; field of view, 10 cm; matrix, 512 × 256; slice thickness, 3 mm; signal averaging, 4; acquiring

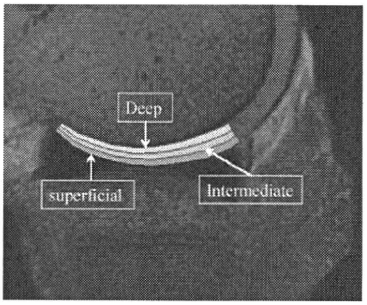

Fig. 2. Sagittal view of the femoral cartilage in the porcine knee, which was subdivided into three zones using custom-made software.

time, 2 min and 35 s). In both sequences, the same sagittal imaging planes were obtained in each examination series using identical axial localizing images.

Image analysis

Data was analyzed using custom-made software (Baum version 1.00; Osaka university, Japan). Sagittal images passing through the middle of the medial and lateral femoral condyles were used. The region of interest (ROI) was manually defined on the weight-bearing area of the medial and lateral femoral cartilages between the anterior and posterior margins of the meniscus based on SPGR images. The ROI was then transferred to the corresponding T2 maps and subdivided into superficial, intermediate, and deep zones with thickness one-third that of the total cartilage, automatically yielding mean T2 values of each subdivided ROI (Fig. 2). Definitions of ROI were repeated twice by a single observer (TS) and the T2 values of each medial and lateral ROI were averaged. Reproducibility between the two measurements was calculated as the coefficient of variation and mean reproducibility were calculated as the root mean square average for all specimens. Reproducibility values of T2 measurements in the superficial, intermediate, and deep zones were 3%, 4%, and 3% in the medial cartilage and 5%, 3%, and 4% in the lateral cartilage, respectively. Inter-observer reproducibility between two observers (TS and IN, an orthopaedic surgeon) for definition of ROI was also evaluated in five knee joints. The reproducibility of T2 measurements in the superficial, intermediate, and deep zones were 5%, 4%, and 5% in the medial cartilage and 4%, 3%, and 3% in the lateral cartilage, respectively.

Joint pressure analysis with pressure-sensitive film

Following MRI, the knee joints were wrapped in gauze soaked in phosphate buffered saline (PBS) solution to be kept moist, and left for 10 h in an unloaded condition at 20°C in the acryl box. Two pieces of pressure-sensitive film (FUJI PRESCALE low sensitivity, FUJIFILM, Japan) were placed between the femur and the meniscus on the medial and lateral sides after making a small opening in the capsule. The incisions allowed access to the posterior root of the lateral or medial meniscus and facilitated inspection of the posterior compartments to confirm consistent placement of the film below the lateral and medial femoral condyle as well as to verify that the film was not folded on itself. Just as in MRI examinations, the joints were mounted in the custom compression device. Neutral loading-1 was applied for the corresponding imaging time. Films were removed, calibrated with a 0.5 cm^2 stamp in a material-testing machine by applying a set of defined loads, and the staining of the film converted into pressure intervals (N) with image analysis. The same pressure analysis was conducted for varus loading. Fukubayashi *et al.* estimated accuracy of Fuji Prescale films within 10%–15%[15], and Wu *et al.* reported the measurement error of the film was approximately 10%[16].

Statistical analysis

T2 values under no loading, neutral loading-1, neutral loading-2, and varus loading conditions at each ROI were compared using a paired *t*-test to estimate the influence of varying compression and knee alignment. Relationships among T2 values in each zone and joint pressure measurements recorded by a pressure-sensitive film were evaluated using Spearman's correlation coefficient. $P < 0.05$ was considered significant.

Results

Under no loading, mean T2 values of the deep, intermediate, and superficial zones were 59.3 ± 3.7 ms, 62.4 ± 7.6 ms, and 67.3 ± 6.4 ms in the medial cartilage, and 62.6 ± 7.5 ms, 64.6 ± 9.2 ms, 71.9 ± 7.8 ms in the lateral cartilage (Table I), respectively. T2 values in the medial and lateral superficial zones had significantly higher values compared to medial and lateral deep zones ($P < 0.05$).

In the medial cartilage, mean T2 values of the deep, intermediate, and superficial zones decreased by 1.4%, 13.0%, and 6.0% under neutral loading-1, and further decreased by 4.3%, 19.3%, and 17.2% under varus loading, compared with the mean T2 values under no loading (Figs. 3 and 4). In the lateral cartilage, these T2 values decreased by 3.9%, 7.7%, and 4.2% under neutral loading-1, but increased by 1.6%, 9.6%, and 7.2% under varus loading (Figs. 3 and 5). There was a significant decrease in T2 values in the intermediate zone of the medial cartilage under both neutral loading-1 and varus loading ($P < 0.05$). In all three zones, changes in T2 time between neutral loading-1 and neutral loading-2 ranged from 0.8% to 3.7%, but the difference was not significant (Table II).

Table I
T2 values in each zone under no loading and each loading condition ($N = 10$)

	No loading	Neutral loading-1			Varus loading		
	Mean T2 (SD)	Mean T2 (SD)	Change (95% CI)	*P*-Value	Mean T2 (SD)	Change (95% CI)	*P*-Value
Medial cartilage							
Deep	59.3 (3.7)	58.4 (5.2)	−1.4 (−5.7, 2.9)	0.68	54.9 (5.2)	−4.3 (−7.3, −1.4)	0.14
Intermediate	62.4 (7.6)	54.4 (7.4)	−13.0 (−17.3, −8.7)	0.03*	46.7 (9.1)	−19.3 (−23.9, −14.6)	0.0005*
Superficial	67.3 (6.4)	63.1 (6.4)	−6.0 (−9.1, −3.0)	0.17	53.4 (5.1)	−17.2 (−19.1, −15.4)	<0.0001*
Lateral cartilage							
Deep	62.6 (7.5)	60.2 (6.1)	−3.9 (−8.0, 0.3)	0.44	63.7 (6.5)	1.6 (−2.8, 6.1)	0.75
Intermediate	64.6 (9.2)	59.6 (8.4)	−7.7 (−10.5, −4.9)	0.22	70.7 (5.6)	9.6 (3.5, 15.6)	0.09
Superficial	71.9 (7.8)	68.8 (9.0)	−4.2 (−7.5, −1.0)	0.43	77.1 (8.5)	7.2 (3.9, 10.5)	0.17

Changes were calculated as (values at each loading condition − values at no loading)/values at no loading × 100.
95% CI: confidence interval.
* Significant difference between values under no loading and each loading condition.

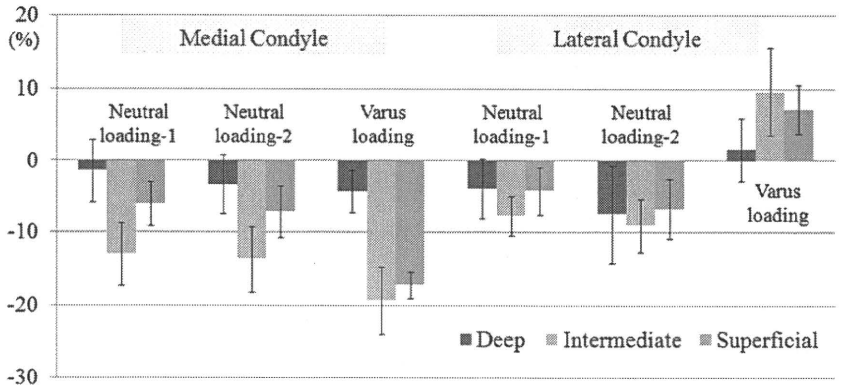

Fig. 3. Change in T2 values (95% confidence interval error bars) at each loading condition. ($N = 10$) Changes were calculated as (values at each loading condition – values at no loading)/values at no loading × 100.

Total contact pressure values at the medial and lateral femoral cartilages were 47 ± 8.4 N and 46 ± 5.1 N under neutral loading-1 and 94 ± 21 N and 35 ± 7.8 N under varus loading (Fig. 6). These values significantly correlated with T2 values in the intermediate (neutral loading-1 and varus loading: $r = -0.64$ and -0.49) and superficial ($r = -0.48$ and -0.55) zones of the medial cartilage, and in the intermediate ($r = -0.48$ and -0.78) and superficial (varus loading: $r = -0.73$) zones of the lateral cartilage (Table III, Fig. 7).

Discussion

Changes in signal intensity and quantitative assessments of MRI in response to static loading were investigated using bone–cartilage plugs in experimental studies[8,9,11,17]. Rubenstein *et al.* examined the MRI appearance of an excised bovine cartilage under static compression[9]. At an initial pressure of 1.10 MPa, they observed a decrease in signal intensity in the thin superficial zone of the cartilage but an increase in the deep zone. This was followed by a gradual decrease in signal intensity along the entire depth of the cartilage as the pressure was increased. At a continuous pressure of 0.69 MPa, using a pressure cell, Kaufman *et al.* observed a reduction in T1 and T2 values in both normal and trypsin-degraded bovine cartilage discs under static pressure[11]. They calculated the permeability of the cartilage as a function of cartilage strain, and showed that the high permeability seen in the uncompressed state decreased progressively with increasing strain. A decrease in T2 values under static loading has been mainly accounted for depth-dependent movement of water content and deformation of the collagen architecture within the cartilage[9,13,18,19]. Approximately 80% of a normal cartilage is water[20], and 94% of this water is freely diffusible and readily exchanges with the intraarticular synovial fluid[21]. On applying static compression onto the cartilage, interstitial water exudes from the cartilage surface or moves to a deeper zone of the cartilage, contributing to depth-specific changes in signal intensity of T2 on MRI[22]. Furthermore, T2 of the articular cartilage is subject to the "magic angle effect" in accordance with the relative position between collagen alignment in the cartilage and direction of the external magnetic field[23]. T2 would change under loading because of altered orientation of collagen fibers relative to the external magnetic field, but the effect of the change is influenced by pressure distribution and original anisotropic collagen fiber architecture along its depth[22]. Reiter *et al.* investigated water compartmentation in cartilage using multiexponential analysis of T2 relaxation data to evaluate anisotropy in the cartilage[24]. Hardy *et al.* demonstrated elastographic method for measuring the spatial variation of compression within articular cartilage[25].

In the present study, the influence of static loading on T2 mapping of the cartilage was investigated using whole animal knee joints retaining all intraarticular structures, capsules, and surrounding muscles. These realistic joint models allowed for static loading under near-physiological conditions unlike excised cartilage specimens, and permitted examining simulated disease conditions (e.g., varus knee alignment). As expected from experimental studies[8,11], a decrease in cartilage T2 occurred in response to static loading in neutral alignment, with remarkable side- and depth-dependent variation in T2 changes; this decrease was more apparent in the medial femorotibial joints. In human knees with neutral alignment, the medial compartment is subjected to higher load than the lateral compartment because of the knee adduction moment in the stance phase[26,27]. Morrison *et al.* investigated the mechanics of knee joint during walking using a force-plate cinephotographic technique, and indicated that the greater part of the joint force was transmitted by the medial condyle[27]. Although there are species-specific variations in knee morphology and biomechanics, the biomechanical status may differ between the medial

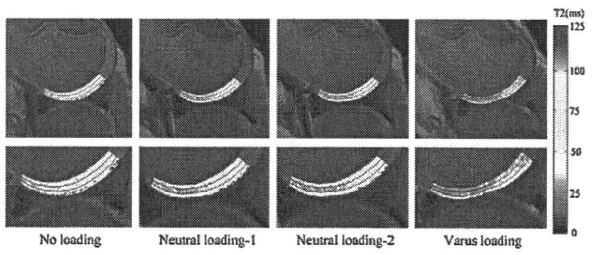

Fig. 4. Representative sagittal MRI of the medial femoral cartilage in the porcine knee at each condition. The femoral cartilage was subdivided into three zones using custom-made software. The lower figures showed the detail of femoral cartilage.

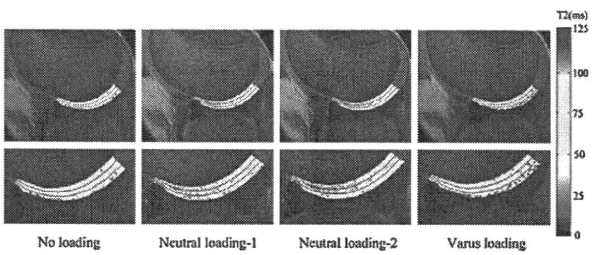

Fig. 5. Representative sagittal MRI of the lateral femoral cartilage in the porcine knee at each condition. The femoral cartilage was subdivided into three zones using custom-made software. The lower figures showed the detail of femoral cartilage.

Table II
T2 values in each zone under neutral loading-1 and neutral loading-2 ($N = 10$)

Zones	Medial cartilage (ms)			Lateral cartilage (ms)		
	Neutral loading-1 (SD)	Neutral loading-2 (SD)	Change (95% CI)	Neutral loading-1 (SD)	Neutral loading-2 (SD)	Change (95% CI)
Deep	58.4 (5.2)	57.4 (5.4)	−1.8 (−3.7, 0.0)	60.2 (6.1)	58.0 (6.9)	−3.7 (−7.4, 0.1)
Intermediate	54.4 (7.4)	53.9 (7.4)	−0.8 (−2.7, 1.1)	59.6 (8.4)	58.8 (9.0)	−1.4 (−3.8, 1.1)
Superficial	63.1 (6.4)	62.6 (7.2)	−1.1 (−2.8, 0.6)	68.8 (9.0)	67.1 (8.9)	−2.6 (−4.3, −0.9)

At neutral loading-2, T2 maps and 3D SPGR images were obtained after compression was continued for 30 min following MR imaging at neutral loading-1, to examine the influence of loading duration on cartilage T2 measurements.
Changes were calculated as (values under neutral loading-2 − values under neutral loading-1)/values under neutral loading-1 × 100.
No significant difference between values under neutral loading-1 and neutral loading-2.

and lateral sides of the knee joint even at neutral alignment showing side-dependent T2 changes under loading.

Decrease in T2 was significantly larger in the intermediate cartilage zone than in the deep cartilage zone in both medial and lateral femorotibial joints. This depth-wise change in cartilage T2 under static loading may be related to different biomechanical functions of the cartilage zones. The deep zone of the cartilage comprises predominantly parallel collagen fibers aligned perpendicular to the subchondral plate (deep zone). The next zone of the cartilage comprises randomly oriented fibers (intermediate zone). The thin superficial zone of the cartilage comprises fibers aligned parallel to the articular surface (superficial zone)[22]. A radially oriented collagen network is responsible for the elastic properties of the cartilage, whereas the tangential arrangement of the collagen network essentially reflects shear forces within the loaded cartilage[28]. Using excised bone-cartilage plugs of juvenile pigs, Gründer *et al.* reported that under static loading MR intensity changed differently in three zones and the MR intensity of radial zone increased in which collagen fibers spread out and the portion of fibers oriented at magic angle with respect to the static magnetic field increased[8]. Rubenstein *et al.* observed an increase of cartilage T2 in the deep zone of excised cartilage plugs under static loading with the effect of increasingly obliquely oriented collagen fibers[9]. In contrast, Visser *et al.* assessed diffusion tensor imaging and cartilage T2 to observe adaptations of collagen fibers to mechanical compression in excised cartilage plugs and demonstrated compression led to the largest decreased T2 value in the superficial and transitional zone[29]. Our result that cartilage T2 values changed in layer-specific manner of three zones under static loading was similar to those previous studies, but predominant trend of increase or decrease of cartilage T2 by loading was different. Cartilage T2 in response to static loading was influenced by several factors, such as deformation of cartilage architecture, extrusion of water content, and relative increase of proteoglycan and collagen content within the cartilage[6,8,9,13,19]. Patterns and severity of those confounding factors under loading may be different between excised cartilage plugs and the whole-knee joint model in our study. Further investigation regarding layer-specific T2 value under loading will be required.

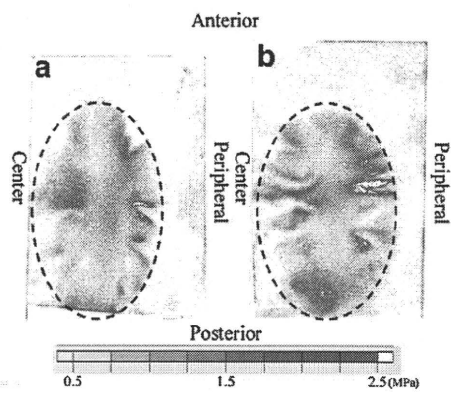

Fig. 6. Representative pressure distributions in pressure-sensitive films inserted under the medial femoral condyle. The color scale at the bottom shows values representing megapascals. (a) Under neutral loading-1 condition. (b) Under varus loading condition. Circle in dotted lines corresponds to a weight bearing area. Note that pressure concentration was shown more severely and diffusely along the medial meniscus under varus loading condition compared with neutral loading-1 condition.

These site-specific changes of cartilage T2 under static loading were remarkable when there was a change in varus alignment (varus loading). Guettler *et al.* investigated femorotibial pressure on eight fresh-frozen cadaveric knees and found that a relatively small degree of varus malalignment caused a dramatic alteration in articular surface contact pressure[30]. Our finding that cartilage T2 was further decreased in the medial joints but increased in the lateral joints under varus loading was in accordance with the biomechanical studies of Guettler *et al.*[30]. Significant correlation with joint pressure measurements and cartilage T2 values in the present study also indicated the usefulness of T2 change under static loading for biomechanical assessment. In patients with knee disorders, increased mechanical stress caused by malalignment is an important risk factor for progression of femorotibial osteoarthritis[26]. T2 mapping under loading may be a potent, non-invasive imaging tool for prognosis of osteoarthritis progression by evaluating altered loading condition imposed on the cartilage resulting from abnormal knee alignment such as varus deformity, and degenerative or traumatic disorders of the meniscus[18].

Cartilage deformation under loading occurs as a function of time and magnitude of load application. Herberhold *et al.* studied deformational behavior of the articular cartilage under static loading of 150% of the body weight with femoropatellar knee imaging *ex vivo*[10]. The deformations of the patellar and femoral cartilages after 8 min of compression were 25%–30% of the final deformation of these cartilages after 214 min of compression. We compared cartilage T2 under the same static loading conditions after 5 min (neutral loading-1) and 30 min (neutral loading-2) of compression to examine the influence of loading duration on cartilage T2 measurements. There was no significant difference in T2 values between neutral loading-1 and neutral loading-2 in any zone. This may indicate that equilibrium of cartilage deformation in response

Table III
Correlation coefficient between T2 values and contact pressure in each zone under neutral loading-1 and varus loading ($N = 10$)

Zones	Neutral loading-1	Slope	*P*-Value	Varus loading	Slope	*P*-Value
Medial cartilage						
Deep	−0.17	−0.11	0.647	−0.12	−0.13	0.741
Intermediate	−0.64	−0.66	0.031*	−0.49	−0.42	0.047*
Superficial	−0.48	−0.47	0.048*	−0.55	−0.53	0.043*
Lateral cartilage						
Deep	−0.23	−0.27	0.533	−0.39	−0.41	0.179
Intermediate	−0.48	−0.59	0.049*	−0.78	−0.67	0.005*
Superficial	−0.41	−0.44	0.184	−0.73	−0.80	0.015*

* Significant correlation between T2 values and contact pressure.